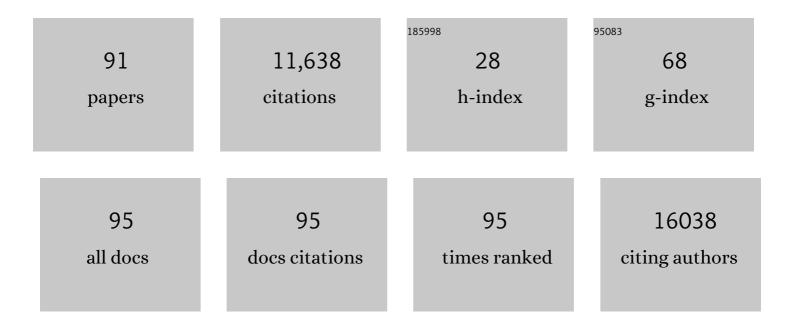
List of Publications by Year in descending order

Source: https://exaly.com/author-pdf/3476567/publications.pdf Version: 2024-02-01



IAMES C GEE

#	Article	IF	CITATIONS
1	Fully Automated Placental Volume Quantification From <scp>3D</scp> Ultrasound for Prediction of Smallâ€forâ€Gestationalâ€Age Infants. Journal of Ultrasound in Medicine, 2022, 41, 1509-1524.	0.8	4
2	Ex vivo MRI and histopathology detect novel iron-rich cortical inflammation in frontotemporal lobar degeneration with tau versus TDP-43 pathology. NeuroImage: Clinical, 2022, 33, 102913.	1.4	17
3	Divergent Histopathological Networks of Frontotemporal Degeneration Proteinopathy Subytpes. Journal of Neuroscience, 2022, 42, 3868-3877.	1.7	4
4	Phases of volume loss in patients with known frontotemporal lobar degeneration spectrum pathology. Neurobiology of Aging, 2022, 113, 95-107.	1.5	5
5	The ANTsX ecosystem for quantitative biological and medical imaging. Scientific Reports, 2021, 11, 9068.	1.6	81
6	Diminishing Efficacy of Prone Positioning With Late Application in Evolving Lung Injury. Critical Care Medicine, 2021, 49, e1015-e1024.	0.4	14
7	Brain MRI Deep Learning and Bayesian Inference System Augments Radiology Resident Performance. Journal of Digital Imaging, 2021, 34, 1049-1058.	1.6	3
8	lmage―versus histogramâ€based considerations in semantic segmentation of pulmonary hyperpolarized gas images. Magnetic Resonance in Medicine, 2021, 86, 2822-2836.	1.9	6
9	Cellular anatomy of the mouse primary motor cortex. Nature, 2021, 598, 159-166.	13.7	117
10	Machine learning suggests polygenic risk for cognitive dysfunction in amyotrophic lateral sclerosis. EMBO Molecular Medicine, 2021, 13, e12595.	3.3	13
11	Anatomical structures, cell types and biomarkers of the Human Reference Atlas. Nature Cell Biology, 2021, 23, 1117-1128.	4.6	68
12	A Precise Method to Evaluate 360 Degree Measures of Optic Cup and Disc Morphology in an African American Cohort and Its Genetic Applications. Genes, 2021, 12, 1961.	1.0	0
13	Reduced longitudinal change in <sup>18</sup> Fâ€flortaucipir PET is associated with clinical phenotype in atypical Alzheimer's disease. Alzheimer's and Dementia, 2021, 17, .	0.4	0
14	Subspecialty-Level Deep Gray Matter Differential Diagnoses with Deep Learning and Bayesian Networks on Clinical Brain MRI: A Pilot Study. Radiology: Artificial Intelligence, 2020, 2, e190146.	3.0	20
15	Spatially Informed CNN for Automated Cone Detection in Adaptive Optics Retinal Images. , 2020, 2020, 1383-1386.		1
16	Artificial Intelligence System Approaching Neuroradiologist-level Differential Diagnosis Accuracy at Brain MRI. Radiology, 2020, 295, 626-637.	3.6	77
17	Minimally interactive placenta segmentation from three-dimensional ultrasound images. Journal of Medical Imaging, 2020, 7, 1.	0.8	6
18	In vivo imaging of canine lung deformation: effects of posture, pneumonectomy, and inhaled erythropoietin. Journal of Applied Physiology, 2020, 128, 1093-1105.	1.2	3

#	Article	IF	CITATIONS
19	Convolutional Neural Network for Automated FLAIR Lesion Segmentation on Clinical Brain MR Imaging. American Journal of Neuroradiology, 2019, 40, 1282-1290.	1.2	61
20	Learning image-based spatial transformations via convolutional neural networks: A review. Magnetic Resonance Imaging, 2019, 64, 142-153.	1.0	30
21	Longitudinal progression of grey matter atrophy in non-amnestic Alzheimer's disease. Brain, 2019, 142, 1701-1722.	3.7	37
22	Effect of Reconstruction Parameters on the Quantitative Analysis of Chest Computed Tomography. Journal of Thoracic Imaging, 2019, 34, 92-102.	0.8	21
23	Deep Learning Applications in Chest Radiography and Computed Tomography. Journal of Thoracic Imaging, 2019, 34, 75-85.	0.8	90
24	Convolutional Neural Networks with Template-Based Data Augmentation for Functional Lung Image Quantification. Academic Radiology, 2019, 26, 412-423.	1.3	51
25	Automated data extraction and ensemble methods for predictive modeling of breast cancer outcomes after radiation therapy. Medical Physics, 2019, 46, 1054-1063.	1.6	8
26	Automatic longitudinal montaging of adaptive optics retinal images using constellation matching. Biomedical Optics Express, 2019, 10, 6476.	1.5	16
27	Shape Decomposition of Foveal Pit Morphology Using Scan Geometry Corrected OCT. Lecture Notes in Computer Science, 2019, 11855, 69-76.	1.0	0
28	Chain-based big data access control infrastructure. Journal of Supercomputing, 2018, 74, 4945-4964.	2.4	23
29	A Retrospective Study of Predictors of Return to Duty versus Medical Retirement in an Active Duty Military Population with Blast-Related Mild Traumatic Brain Injury. Journal of Neurotrauma, 2018, 35, 991-1002.	1.7	20
30	V-Chain: A Blockchain-Based Car Lease Platform. , 2018, , .		7
31	A Blockchain-based Architecture Framework for Secure Sharing of Personal Health Data. , 2018, , .		55
32	Longitudinal structural gray matter and white matter MRI changes in presymptomatic progranulin mutation carriers. Neurolmage: Clinical, 2018, 19, 497-506.	1.4	21
33	A new scale for the assessment of conjunctival bulbar redness. Ocular Surface, 2018, 16, 436-440.	2.2	11
34	2D Modeling and Correction of Fan-Beam Scan Geometry in OCT. Lecture Notes in Computer Science, 2018, 11039, 328-335.	1.0	1
35	Development and Evaluation of Semiautomated Quantification of Lissamine Green Staining of the Bulbar Conjunctiva From Digital Images. JAMA Ophthalmology, 2017, 135, 1078.	1.4	8
36	Automated Segmentation of the Choroid inÂEDI-OCT Images with Retinal Pathology Using Convolution Neural Networks. Lecture Notes in Computer Science, 2017, 10554, 177-184.	1.0	26

JAMES C GEE

#	Article	IF	CITATIONS
37	Tidal changes on CT and progression of ARDS. Thorax, 2017, 72, 981-989.	2.7	39
38	Joint alignment of multispectral images via semidefinite programming. Biomedical Optics Express, 2017, 8, 890.	1.5	10
39	Multimodal Image Alignment via Linear Mapping between Feature Modalities. Journal of Healthcare Engineering, 2017, 2017, 1-6.	1.1	8
40	Retinal Image Denoising via Bilateral Filter with a Spatial Kernel of Optimally Oriented Line Spread Function. Computational and Mathematical Methods in Medicine, 2017, 2017, 1-13.	0.7	20
41	Multi-modal automatic montaging of adaptive optics retinal images. Biomedical Optics Express, 2016, 7, 4899.	1.5	49
42	Arterial spin labeling perfusion predicts longitudinal decline in semantic variant primary progressive aphasia. Journal of Neurology, 2016, 263, 1927-1938.	1.8	23
43	Novel human intervertebral disc strain template to quantify regional threeâ€dimensional strains in a population and compare to internal strains predicted by a finite element model. Journal of Orthopaedic Research, 2016, 34, 1264-1273.	1.2	18
44	White matter hyperintensities are more highly associated with preclinicalÂAlzheimer's disease than imaging and cognitive markers ofÂneurodegeneration. Alzheimer's and Dementia: Diagnosis, Assessment and Disease Monitoring, 2016, 4, 18-27.	1.2	71
45	Computational analysis in epilepsy neuroimaging: A survey of features and methods. NeuroImage: Clinical, 2016, 11, 515-529.	1.4	68
46	The DTI Challenge: Toward Standardized Evaluation of Diffusion Tensor Imaging Tractography for Neurosurgery. Journal of Neuroimaging, 2015, 25, 875-882.	1.0	147
47	Parenchymal texture analysis in digital mammography: robust texture feature identification and equivalence across devices. Journal of Medical Imaging, 2015, 2, 024501.	0.8	19
48	Eigenanatomy: Sparse dimensionality reduction for multi-modal medical image analysis. Methods, 2015, 73, 43-53.	1.9	15
49	Parenchymal texture analysis in digital mammography: A fully automated pipeline for breast cancer risk assessment. Medical Physics, 2015, 42, 4149-4160.	1.6	91
50	Measuring sparse temporal-variation for accurate registration of dynamic contrast-enhanced breast MR images. Computerized Medical Imaging and Graphics, 2015, 46, 73-80.	3.5	7
51	Plasticity of the human visual system after retinal gene therapy in patients with Leber's congenital amaurosis. Science Translational Medicine, 2015, 7, 296ra110.	5.8	51
52	Decomposing cerebral blood flow MRI into functional and structural components: A non-local approach based on prediction. NeuroImage, 2015, 105, 156-170.	2.1	13
53	Semiautomatic segmentation of longitudinal computed tomography images in a rat model of lung injury by surfactant depletion. Journal of Applied Physiology, 2015, 118, 377-385.	1.2	20
54	Linear Associations between Clinically Assessed Upper Motor Neuron Disease and Diffusion Tensor Imaging Metrics in Amyotrophic Lateral Sclerosis. PLoS ONE, 2014, 9, e105753.	1.1	38

#	Article	IF	CITATIONS
55	High Resolution Magnetic Resonance Imaging for Characterization of the Neuroligin-3 Knock-in Mouse Model Associated with Autism Spectrum Disorder. PLoS ONE, 2014, 9, e109872.	1.1	36
56	The Insight ToolKit image registration framework. Frontiers in Neuroinformatics, 2014, 8, 44.	1.3	462
57	Reproducibility of graph metrics of human brain structural networks. Frontiers in Neuroinformatics, 2014, 8, 46.	1.3	33
58	Cortical parcellation for neonatal brains. , 2014, , .		2
59	Landmark matching based retinal image alignment by enforcing sparsity in correspondence matrix. Medical Image Analysis, 2014, 18, 903-913.	7.0	32
60	Relating brain anatomy and cognitive ability using a multivariate multimodal framework. NeuroImage, 2014, 99, 477-486.	2.1	29
61	Large-scale evaluation of ANTs and FreeSurfer cortical thickness measurements. NeuroImage, 2014, 99, 166-179.	2.1	560
62	Subject-specific functional parcellation via Prior Based Eigenanatomy. Neurolmage, 2014, 99, 14-27.	2.1	13
63	An automated drusen detection system for classifying age-related macular degeneration with color fundus photographs. , 2013, , .		19
64	Anatomically-Constrained PCA for Image Parcellation. , 2013, , .		2
65	White Matter Disease Correlates with Lexical Retrieval Deficits in Primary Progressive Aphasia. Frontiers in Neurology, 2013, 4, 212.	1.1	29
66	Optic Disc and Cup Segmentation from Color Fundus Photograph Using Graph Cut with Priors. Lecture Notes in Computer Science, 2013, 16, 75-82.	1.0	39
67	A Generative Model for OCT Retinal Layer Segmentation by Integrating Graph-Based Multi-surface Searching and Image Registration. Lecture Notes in Computer Science, 2013, 16, 428-435.	1.0	10
68	Partial sparse canonical correlation analysis (PSCCA) for population studies in medical imaging. , 2012, , .		1
69	Retrospective illumination correction of retinal fundus images from gradient distribution sparsity. , 2012, , .		13
70	Reconstruction of the human hippocampus in 3D from histology and high-resolution ex-vivo MRI. , 2012, 2012, 294-297.		7
71	A reproducible evaluation of ANTs similarity metric performance in brain image registration. NeuroImage, 2011, 54, 2033-2044.	2.1	3,535
72	An Open Source Multivariate Framework for n-Tissue Segmentation with Evaluation on Public Data. Neuroinformatics, 2011, 9, 381-400.	1.5	515

#	Article	IF	CITATIONS
73	Multiscale analysis revisited: Detection of drusen and vessel in digital retinal images. , 2011, , .		7
74	Cranio-maxillofacial surgery simulation based on pre-specified target face configurations. Journal of Zhejiang University: Science C, 2010, 11, 504-513.	0.7	2
75	N4ITK: Improved N3 Bias Correction. IEEE Transactions on Medical Imaging, 2010, 29, 1310-1320.	5.4	4,205
76	Accurate registration of dynamic contrast-enhanced breast mr images with robust estimation and linear programming. , 2010, , .		4
77	Estimation of image bias field with sparsity constraints. , 2010, , .		15
78	A framework for craniofacial surgery simulation based on pre-specified target face configurations. , 2009, , .		0
79	Registration based cortical thickness measurement. NeuroImage, 2009, 45, 867-879.	2.1	217
80	Topological Repairing of 3D Digital Images. Journal of Mathematical Imaging and Vision, 2008, 30, 249-274.	0.8	35
81	Robust regularization for the estimation of intra-voxel axon fiber orientations. , 2008, , .		2
82	Atlas-guided probabilistic diffusion-tensor fiber tractography. , 2008, , .		5
83	Multivariate segmentation of brain tissues by fusion of MRI and DTI data. , 2008, , .		7
84	Branching medial models for cardiac shape representation. , 2008, , .		4
85	Surface-based modeling of white matter fasciculi with orientation encoding. , 2008, , .		1
86	Spatial correspondence based asymmetry analysis in FMRI. , 2008, , .		0
87	Structure-Specific Statistical Mapping of White Matter Tracts using the Continuous Medial Representation. , 2007, , .		24
88	CONSTRAINED QUADRILATERAL MESHES OF BOUNDED SIZE. International Journal of Computational Geometry and Applications, 2005, 15, 55-98.	0.3	8
89	Alzheimer's disease and frontotemporal dementia exhibit distinct atrophy-behavior correlates. Academic Radiology, 2003, 10, 1392-1401.	1.3	37
90	Characterization of regional pulmonary mechanics from serial magnetic resonance imaging data1. Academic Radiology, 2003, 10, 1147-1152.	1.3	57

#	Article	IF	CITATIONS
91	Performance Evaluation of Medical Image Processing Algorithms. Series in Machine Perception and Artificial Intelligence, 2002, , 143-159.	0.1	0